Journal of Nuclear Medicine, published on July 20, 2017 as doi:10.2967/jnumed.117.193854

Imaging chemokine receptor CXCR4 in chronic infection of the bone with ^{68}Ga-Pentixafor-PET/CT – first insights.

Running title: ^{68}Ga-Pentixafor-PET/CT in bone infection

Caroline Bouter[1]*, Birgit Meller[1], Carsten O. Sahlmann[1], Wieland Staab[2], Hans J. Wester[3], Saskia Kropf[4], Johannes Meller[1]

[1]Department of Nuclear Medicine, Georg-August-University Göttingen, Göttingen, Germany

[2]Department of Radiology, Georg-August-University Göttingen, Göttingen, Germany

[3]Pharmaceutical Radiochemistry, Technical University of Munich

, Walther-Meißner-Str.3, 85748, Garching, Germany.

[4]SCINTOMICS GmbH, Lindach 4, 82256 Fuerstenfeldbruck, Germany

*** Corresponding author:**

Caroline Bouter, Department of Nuclear Medicine, Resident

Georg-August-University Göttingen, Robert-Koch-Str. 40, 37075, Göttingen, Germany

Tel. +49551398511, Fax +49551398526

caroline.bouter@med.uni-goettingen.de

Word count: 4989

ABSTRACT

Due to its role in infection and inflammatory processes the chemokine receptor CXCR4 might be a potent target in imaging of infectious and inflammatory diseases. The aim of this pilot study was to determine whether the CXCR4 ligand ^{68}Ga-Pentixafor is suitable for imaging chronic infection of the bone.

Methods: The study comprises 14 patients with suspected infection of the skeleton that underwent ^{68}Ga-Pentixafor-Positron emission tomography/computed tomography (PET/CT) between 04/2015 and 02/2017 in our facility. ^{68}Ga-Pentixafor-PET/CT results were retrospectively evaluated against a histological, bacteriological and clinical standard. Results were also compared to available bone scintigraphy, white blood cell (WBC) scintigraphy and ^{18}F-FDG-PET/CT.

Results: ^{68}Ga-Pentixafor-PET/CT was positive in 9/14 patients. Diagnoses included osteitis/osteomyelitis of peripheral bone, osteomyelitis of the maxilla and infected endoprostheses. Target-background ratios were 5,1 to 15 (mean 8,7). 8/9 cases were true positive confirmed by pathology, bacteriology or clinical observation. All negative cases were confirmed true negative by other imaging modalities and follow up.

Conclusion: Imaging of CXCR4 expression with ^{68}Ga-Pentixafor-PET/CT appears suitable for diagnosing chronic infection of the skeleton. Findings of this study reveal a possible diagnostic gain in

suspected chronic infections that are difficult to diagnose by other imaging modalities.

Key words: osteomyelitis, PET/CT, pentixafor, CXCR4, molecular imaging

INTRODUCTION

Diagnosis of skeletal infections displays a clinical and diagnostic challenge as patients present with a variety of clinical symptoms. The diagnostic workup usually includes a combination of clinical, laboratory and imaging findings. Whereas acute posttraumatic infections (first 2 weeks after trauma/surgery) are usually diagnosed by clinical examination, common signs of infection might be absent in later phases and additional diagnostics are crucial (*1*). In acute osteomyelitis the innate immune response, mainly including neutrophils and macrophages, is essential. Chronic osteomyelitis shows a more heterogeneous distribution of leukocytes in which components of the adaptive immune response are leading. Even though neutrophils can still play a role in chronic phases, they can be absent in some situations and lymphocytes might become the major fraction of immune cells (*2*). Due to its role in inflammatory processes and its high expression levels on lymphocytes, the chemokine receptor CXCR4 might be a potent target in imaging chronic infectious diseases. Various tumor cells overexpress CXCR4 and the radiolabeled CXCR4-ligand ^{68}Ga-Pentixafor, developed in 2011, has shown to be useful in imaging multiple myelomas, gliomas and small cell lung cancer (*3-10*).

The aim of this proof-of-principle study was the determination whether ^{68}Ga-Pentixafor-PET/CT is a suitable method in imaging chronic infectious diseases of the skeleton.

PATIENTS AND METHODS

Patients

A total of 27 consecutive patients that underwent ^{68}Ga-Pentixafor-PET/CT in our facility between April 2015 and February 2017 were evaluated retrospectively. 13 patients were excluded as clinical questions were carcinomas or large vessel vasculitis and did not include infection of the bone. Therefore, the study comprises 14 consecutive patients (7 females and 7 males aged 19-78, mean age 57) with suspected osteomyelitis. The suspected diagnosis was decided by clinical or laboratory results in the department of orthopedics or oral and maxillofacial surgery and imaging of infection of the bone was requested. Patients were presented to our department after a routine workflow in which bone scintigraphy is the first line of nuclear medicine imaging. The second step of the routine workflow includes leukocyte imaging. In each case the use of either WBC-imaging and/or ^{68}Ga-Pentixafor-PET/CT was discussed with the referring colleagues and the most suitable method was chosen.

All patients were in a post-interventional stage. Suspected diagnoses included: postoperative osteitis/osteomyelitis of peripheral bone (n=2), postoperative spondylitis (n=3), postinterventional osteitis/osteomyelitis of maxillofacial bone (n=4) and infections of endoprostheses (n=5).

^{68}Ga-Pentixafor-PET/CT was performed 2-103 (mean 20) months after the last surgical intervention. ^{68}Ga-Pentixafor-PET/CT results were evaluated by histology, bacteriology, C-reactive protein levels and clinical follow up. If available, results of bone scan, WBC-scan and ^{18}F-FDG PET/CT were compared to ^{68}Ga-Pentixafor-PET/CT results.

All procedures involving human participants were in accordance with the ethical standards of the institutional and/or national research committee and with the 1964 Helsinki declaration and its later amendments or comparable ethical standards. The institutional review board approved this retrospective study. All patients signed an informed consent.

Radiochemistry

Radiolabeling of 16 nmol Pentixafor peptide (Scintomics, Fuerstenfeldbruck, Germany) was performed with median 1200 (600-2000) MBq ^{68}GaCl3 (^{68}Ge/^{68}Ga-Generator (iThemba Labs, Cape Town, South Africa)) in a GRP™ Module (Scintomics, Fuerstenfeldbruck, Germany) using the cationic purification method according to GMP quality standards. Radiochemical purity was determined by thin-layer chromatography and high-performance liquid chromatography (*11,12*). Peptide amount for each patient was restricted to 8 nmol Pentixafor.

PET/CT

^{68}Ga-Pentixafor-PET/CT was performed on a Philips Gemini TF16 PET/CT-scanner (Philips Medical Systems, Cleveland, OH, USA) with a 144x144 matrix with 4 mm slice thickness and low-dose-CT with a 512x512 matrix with 2 mm slice thickness for attenuation correction (CTAC-SG algorithm). The reconstruction was performed using the LOR-TF-RAMLA ("BLOB-OS-TF") algorithm.

^{68}Ga-Pentixafor-PET/CT was performed in all patients 60 minutes after injection of 166-300 MBq (mean 245 MBq) ^{68}Ga-Pentixafor. Additionally, three patients were scanned using a biphasic protocol (30 and 60 minutes) and two patients were scanned at three different time points (30, 60 and 90 minutes) in order to determine the optimal time point for ^{68}Ga-Pentixafor-PET/CT imaging. Later time points were not studied due to unfavorable count statistics.

A diagnostic CT-scan without the use of contrast agent was performed of the area of interest in all patients. A nuclear medicine physician and a radiologist separately reviewed images. ^{68}Ga-Pentixafor uptake was evaluated visually and maximum standardized uptake values (SUV_{max}) were ascertained for semi-quantitative analysis (SUV=r(a'/w) r=the activity concentration [kBq/ml] measured by the PET scanner within a region of interest, a'=amount of injected radiolabeled FDG [kBq], w=weight of the patient [g]). SUV_{mean} values of contralateral peripheral bone uptake were measured within a standardized rectangle region (25

cm^2). Furthermore, target-background ratios (TBR) were calculated as surrogate marker for lesion-contrast as follows: SUV_{max}(lesion)/SUV_{mean}(background).

Interpretation of findings

^{68}Ga-Pentixafor-PET/CT was positive if the uptake showed higher intensity than the surrounding tissue outside the physiologically distribution. ^{68}Ga-Pentixafor-PET/CT findings were true positive (TP) when histology, bacteriology, laboratory or indisputable macroscopic findings in clinical follow up confirmed the PET/CT result. False positive (FP) findings included PET/CT with an abnormal ^{68}Ga-Pentixafor uptake that could not be confirmed by other imaging methods (Magnetic Resonance Imaging (MRI), X-Ray) and clinical or laboratory follow up. True negative (TN) findings included ^{68}Ga-Pentixafor-PET/CT with physiological uptake that did not show any pathology in other modalities and clinical follow up, C-reactive protein (CRP) or bacteriology confirmed findings. False negative finding was defined as PET/CT with physiological uptake that showed pathologies in other imaging methods or follow up. Non-attenuation corrected PET images were additionally reviewed as attenuation correction might mimic increased tracer uptake in implants.

The assessment of the results, obtained by bone scan, WBC-scan and ^{18}F-FDG-PET/CT was determined applying the same

principles und methods as used in the evaluation of ^{68}Ga-Pentixafor-PET/CT.

Statistical analysis

All data are given as means ± standard error. Unpaired t-test and linear regression was used for statistical evaluation. Data was analyzed for normal distribution. Grubbs' test was used in order to identify statistic outliers and one significant statistic outlier was removed ($p<0.05$) in Supplemental Figure 1. All statistics were calculated using Microsoft Excel (Microsoft Corp., Redmond, WA, USA) or GraphPad Prism version 6.0e for Mac (GraphPad Software, San Diego, CA, USA).

RESULTS

^{68}Ga-Pentixafor-PET/CT results

^{68}Ga-Pentixafor-PET/CT was positive in 9/14 patients. ^{68}Ga-Pentixafor-PET/CT results included: osteitis/osteomyelitis of peripheral bone (n=3), osteomyelitis of the maxilla or mandibula (n=2), spondylodiscitis and infected endoprostheses (n=4).

SUVmax ranged between 2.2 and 4.5 (mean 3.3). TBR were 5.1 to 15 (mean 8.7). In 5 cases a multiphasic protocol was used for image acquisition. In three of these cases ^{68}Ga-Pentixafor-PET/CT was positive. TBR did not significantly differ between 30, 60 and 90 minutes after injection of ^{68}Ga-Pentixafor.

^{68}Ga-Pentixafor-PET/CT results were confirmed in 8/9 PET/CT-positive patients by pathology (n=3), bacteriology (n=3) and clinical follow up (n=2) and therefore TP. Pathology confirmed chronic lymphocytic osteomyelitis in three cases. Bacteriology showed *Staphylococcus aureus* on an external fixator, on a partial knee replacement and on a spacer of a removed knee arthroplasty. One patient showed a purulent fistula surrounding a metatarsophalangeal prosthesis in follow up. The prosthesis was removed afterwards and CRP values normalized postoperatively. A histological or bacteriological examination of the prosthesis was not performed (figure 1). The remaining patient showed an infected

knee endoprosthesis in ^{68}Ga-Pentixafor-PET/CT and CRP normalized after removal of the prosthesis.

One ^{68}Ga-Pentixafor-PET/CT-positive patient was FP. MRI showed a necrotic plasmacytoma in a vertebral body instead of a spondylitis. This patient initially showed a positive CRP that persisted during follow-up (figure 2).

Results of ^{68}Ga-Pentixafor-PET and the diagnostic CT were concordant in 4/9 cases. Remaining 5 cases were negative in the CT scan whereas PET was positive.

CRP was initially positive in 6/8 TP cases ranging between 10.7 and 167 mg/l (mean 46.2 mg/l) and normalized in all TP patients during follow-up. SUV_{max} did not correlate with CRP levels (r=0.002, Supplemental Figure 1).

^{68}Ga-Pentixafor-PET/CT was negative in 5/14 patients. PET/CT results were confirmed by follow up with indisputably results (n=5) and therefore TN. Final diagnoses included: broken screws in a spondylodesis (n=2), aseptic loosening of a knee endoprosthesis (n=2) and post-interventional aseptic changes of the mandible.

Results of ^{68}Ga-Pentixafor-PET and the diagnostic CT were concordant in all 5 cases.

Sensitivity of ^{68}Ga-Pentixafor-PET/CT was 89% and specificity was 83%.

Table 1 shows patient characteristics, PET/CT results, final diagnoses and CRP of ^{68}Ga-Pentixafor-PET/CT-positive patients. Table 2 summarizes results and characteristics of ^{68}Ga-Pentixafor-PET/CT-negative patients.

Other nuclear medicine imaging methods (table 3).

Three-phase bone scintigraphy was performed in 11/14 patients. All scintigraphies were positive. Results were confirmed TP in 7/11 patients by pathology (n=3) or bacteriology (n=4). Remaining 4 patients were FP as results were not confirmed in follow up.

^{18}F-FDG-PET/CT was performed in 4 patients. ^{18}F-FDG-PET/CT was TN in one case with suspected spondylodiscitis. 3 cases were positive in ^{18}F-FDG-PET/CT showing osteitis/osteomyelitis of the peripheral bone (n=2) and a spondylodiscitis. SUV_{max} ranged between 3,2 and 7 (mean 5,6). TBR was 4,5 to 17,5 (mean 10,5). There were no significant differences between TBR in ^{68}Ga-Pentixafor-PET/CT and ^{18}F-FDG-PET/CT (p=0,65). Whereas the osteitis/osteomyelitis cases were TP (proven by bacteriology and pathology) the spondylodiscitis case was FP showing a necrotic plasmocytoma in MRI. The distribution pattern of FDG was comparable to the pattern of Pentixafor uptake. Except of one case with a Pilon fracture of the tibia that showed additional FDG-uptake around bone canals of an external fixator with a SUV_{max} of 2,2. ^{68}Ga-Pentixafor-PET/CT was TN around these bone canals.

WBC scintigraphy was performed in 7 cases (^{111}In-oxine labeled leukocyte scintigraphy (n=6) and ^{99m}Tc-besilesomab). Scintigraphies were true positive in 2/7 cases proven by bacteriology. ^{111}In-oxine scintigraphy showed an infected knee resurfacing in one case and ^{99m}Tc-besilesomab an osteitis after a knee spacer implantation. Both cases were also positive in ^{68}Ga-Pentixafor-PET/CT. However, ^{68}Ga-Pentixafor-PET/CT revealed a distinct osteomyelitis in the patients with the knee spacer implantation, as proven by bacteriology, in which ^{99m}Tc-besilesomab only showed osteitis (figure 3).

In the remaining 5/7 cases WBC-scintigraphies (using ^{111}In-oxine labeled leukocytes) were negative. Two of these cases were false negative confirmed by pathology. Remaining 2 cases were TN confirmed by follow up.

Other imaging methods

MRI was performed in 2 patients. In one case it showed a necrotic plasmocytoma, which was FP in ^{68}Ga-Pentixafor-PET/CT and ^{18}F-FDG-PET/CT, as described above (figure 2). The second case showed a negative MRI with limitations by multiple artefacts due to an external fixator. The patient was TP in ^{68}Ga-Pentixafor-PET/CT showing an osteitis of the femur.

DISCUSSION

Data presented here show the usefulness of ^{68}Ga-Pentixafor-PET/CT in imaging chronic skeletal infections.

Ligand-CXCR4-interactions activate the mitogen-activated protein kinase and phosphoinositid-3 kinase signaling pathway altering cell adhesion, migration and homing of T-and B-lymphocytes, macrophages, neutrophils and eosinophils. CXCR4 is essential for leukocyte trafficking to the site of infection (*13-16*). The only known CXCR4 ligand CXCL12 plays a crucial role in inflammatory diseases like rheumatoid arthritis. 78-88% of T-lymphocytes in the peripheral blood and more than 90% of post-migrational T-cells express CXCR4 (*17-19*). RNA-expression levels also identified lymphocytes as the major CXCR4-expressing mature cell fraction in tissues of the immune system (*20*). Up-and down regulation of CXCR4 expression is differentially on neutrophils, monocytes and lymphocytes modulated by TNF-α and INF-γ (*19,21*). As chronic osteomyelitis can, in certain situations, mainly include lymphocytes on the site of infection a specific tracer should be able to detect lymphocytes and therefore CXCR4 is a promising target for imaging chronic infection of the bone (*2*).

Imaging of skeletal infection can be a challenging situation. Radiological imaging, mainly X-ray or CT, display the first line of imaging methods in suspected skeletal infections. However,

several pitfalls have to be taken into account. X-ray, MRI and CT imaging is aggravated by metal implants due to artefacts and early stages of chronic infection might be missed as sequester or fistulas might not have been formed yet.

Several nuclear medicine imaging methods are established in imaging suspected infection of the bone including conventional bone scintigraphy, WBC imaging and ^{18}F-FDG-PET/CT.

Conventional bone scintigraphy is highly sensitive but has a limited specificity as a variety of conditions beside osteomyelitis show an altered bone metabolism and positive bone scintigraphy (*22*). In our study, bones scintigraphy, if available, was positive in all patients. However, it was FP in 36% of cases. WBC imaging (labeled leukocytes and anti-granulocyte antibodies) shows unfavorable low sensitivity and specificity in the axial skeleton (*23*). Even in the diagnosis of infection in the peripheral skeleton sensitivity and specificity are suboptimal. In a multinational, phase III clinical study in 22 European centers comparing anti-granulocyte imaging with ^{99m}Tc-besilesomab and ^{99m}Tc-labelled white blood cells in patients with peripheral osteomyelitis sensitivity of labeled WBC was only 59% and of ^{99m}Tc-besilesomab 75%. Specificity of labeled WBC was 80% and of ^{99m}Tc-besilesomab 72% (*24*). Furthermore, Ivancevic *et al.* (2002) displayed problems with an anti-granulocyte antibody Fab' fragment in low-grade

chronic bone infections. As neutrophil components of infection are not always present in chronic osteomyelitis the use of labeled WBC may be of limited value in some patients (*25*).

The use of hybrid imaging techniques combining metabolic information with anatomical details can improve both, sensitivity and specificity with a diagnostic gain of up to 48% compared to SPECT (*26-28*).

In a meta-analysis including a total of 163 cases, ^{18}F-FDG-PET/CT was the most sensitive technique in imaging chronic osteomyelitis in the central and peripheral skeleton with a sensitivity of 96% and specificity of 91% (*29*). Results were confirmed by Jamar *et al.* (2013) with a diagnostic accuracy of 95% in available data (a total of 287 cases) (*30*). Despite of these advantages, ^{18}F-FDG-PET/CT shows limitations in early posttraumatic situations and in infected endoprostheses. Within first 3 months after surgery the formation of granulomatous tissue complicates diagnostics of osteomyelitis with possible false positive results (*31*). In the literature those patients are rarely included which might be a possible bias in available data. For example, Guhlmann *et al.* (1998) evaluated ^{18}F-FDG-PET/CT and anti-granulocyte antibody scintigraphy in a prospective setting in 51 patients with suspected osteomyelitis. Study design excluded all patients that underwent bone surgery within the last 2 years. However, the study showed

an excellent diagnostic accuracy for ^{18}F-FDG-PET/CT in both, peripheral (95%) and axial skeleton (93%). Including patients within the first 3 month of surgery might significantly lower those numbers. Endoprostheses also induce the formation of reactive granulation tissue reducing specificity of ^{18}F-FDG-PET/CT (*32,33*). In a review of van der Bruggen et al. (2010) sensitivity and specificity widely varied in patients with orthopedic implant infections (sensitivity from 28% to 91%; specificity from 9% to 97%) (*34*).

Therefore, several clinical situations might profit from an additional PET/CT tracer primary imaging lymphocytes: as early posttraumatic osteomyelitis, infected endoprostheses and osteomyelitis of the axial skeleton. These situations are challenging and require the utmost in diagnostic accuracy. In our study patients with exactly these clinical questions that are difficult to diagnose, normally not included in pilot studies, were true positive with ^{68}Ga-Pentixafor-PET/CT. Four patients were diagnosed TP with infected endoprostheses, two patients with posttraumatic chronic peripheral osteomyelitis and two with chronic osteomyelitis of the jaws. In this retrospective evaluation only one patient with suspected osteomyelitis was presented at our facility for ^{68}Ga-Pentixafor-PET/CT in the early postinterventional phase 2 month after surgery. This patient was TP. However, results of one

patient are not enough to speculate whether ^{68}Ga-Pentixafor-PET/CT might resolve this issue.

Interestingly, ^{68}Ga-Pentixafor uptake was independent from CRP levels in our study as CRP-negative cases also showed sufficient uptake. This might be an added value of Pentixafor as CRP results can be heterogeneous in chronic osteomyelitis and infection of endoprostheses. Michail et al. described a sensitivity of CRP in osteomyelitis of 85% (*35*).

^{68}Ga-Pentixafor-PET/CT showed high TBR comparable to FDG. High TBR is essential for diagnostics in nuclear medicine helping distinguishing pathologies from physiological tracer uptake. Previous studies of various malignancies also showed high TBR and first approaches of CXCR4-directed endoradiotherapy were recently demonstrated (*36*).

One patient with suspected spondylodiscitis was FP for skeletal infection in our study. According to the initial clinical investigators in our facility, a spondylodiscitis was suggested and CT also showed affection of two consecutive vertebrae in this patient. However, retrospectively ^{68}Ga-Pentixafor-uptake was increased in multiple vertebrae pointing to a hematopoietic disease. MRI showed a plasmocytoma in multiple vertebrae. The patient was ruled FP as increased uptake was not confirmed an infection. In the pathophysiology of plasmocytomas CXCR4 plays an essential role

recruiting malignant cells to the bone marrow showing a strong correlation between CXCR4/CXCL12 activation and bone infiltration (*37,38*). Earlier studies also demonstrated the suitability of ^{68}Ga-Pentixafor in PET/CT imaging in plasmocytoma patients emphasizing CXCR4 as a potential target in plasmocytoma therapy (*5,36,39*).

All patients that were negative in ^{68}Ga-Pentixafor-PET/CT were TN assuming a good negative predictive value of the method. Within the group of TN patients even situations that are difficult to image as post-interventional patients or patients with endoprostheses were diagnosed correctly pointing out that the method might be valuable in exclusion diagnostics.

^{18}F-FDG-PET/CT results were comparable to ^{68}Ga-Pentixafor-PET/CT results in our study. Distribution pattern and TBR of FDG and Pentixafor were comparable within the lesions. However, in one osteomyelitis case with a Pilon fracture of the tibia an additional uptake of FDG was present around the bone canals of an external fixator whereas no CXCR4-expression was detected in those areas. The case with suspected spondylodiscitis was FP in ^{18}F-FDG-PET/CT and ^{68}Ga-Pentixafor-PET/CT as both CXCR4 and GLUT1 are known to be overexpressed in plasmocytomas. In this case MRI imaging was decisive.

Furthermore, our study displays known issues with the diagnostic accuracy of ^{111}In-oxine-leukocyte scintigraphy in chronic osteomyelitis of the axial skeleton (*40-42*). A meta-analysis of Termaat *et al.* (2005) showed that leukocyte scintigraphy of the axial skeleton was the least sensitive of the evaluated imaging methods (*29*). Several mechanisms are supposed to cause a loss of sensitivity. First the low TBR between early neutrophil infection and bone marrow activity; second the presence of unspecific 'cold lesions' which are assumed being caused by blood vessel compression or microthrombotic occlusion (*29*). In our study the case with osteomyelitis of the mandible was not detected by ^{111}In-oxine leukocyte scintigraphy but ^{68}Ga-Pentixafor-PET/CT was TP (figure 4). Earlier studies focusing on bone scintigraphy and WBC-scintigraphy in acute and chronic osteomyelitis of the jaw showed high sensitivity of a combination of both methods in acute osteomyelitis decreasing in chronic infections (*43,44*).

^{99m}Tc-besilesomab detected an osteitis after a knee spacer implantation but in a smaller extend than ^{68}Ga-Pentixafor-PET/CT that clearly showed a distinct osteomyelitis. It is suggested, that the small ^{68}Ga-Pentixafor molecule is more effective in accumulation at the site of infection, compared to the slow kinetics of a complete IgG-antibody.

In this study, we were able to display a proof of principle of ^{68}Ga-Pentixafor-PET/CT in chronic skeletal infections. ^{68}Ga-Pentixafor-PET/CT seems to detect CXCR4-expressing lymphocytes at the site of infection. Hypothetical advantages of ^{68}Ga-Pentixafor might be imaging of chronic infections in endoprosthesis (no uptake in foreign body granulomas), osteomyelitis of the axial skeleton (which are often pure lymphocytic infections) and early stages of posttraumatic infection (lymphocytes are not predominant elements of bone healing).

Limitations of our studies are the relatively small sample size and the retrospective setting. Further clinical and pre-clinical studies on ^{68}Ga-Pentixafor-PET/CT in skeletal infections have to be carried out.

CONCLUSION

^{68}Ga-Pentixafor-PET/CT is a suitable method for imaging chronic infection of the skeleton. It might provide a diagnostic gain against other established methods in axial bone infections, early postoperative osteomyelitis and periprosthetic infections as lymphocytic infiltration can be imaged specifically.

AUTHOR DISCLOSURE STATEMENT

Saskia Kropf and Hans-Jürgen Wester are shareholders of SCINTOMICS, Germany. No other potential conflict of interest

relevant to this article was reported. All other authors declare that no competing financial interests exist.

REFERENCES:

1. Lew DP, Waldvogel FA. Osteomyelitis. *Lancet.* 2004;364:369-379.

2. Marais L, Ferreira N, Aldous C, le Roux T. The pathophysiology of chronic osteomyelitis. *SA Orthopaedic Journal.* 2013;12:14-18.

3. Spano JP, Andre F, Morat L, et al. Chemokine receptor CXCR4 and early-stage non-small cell lung cancer: pattern of expression and correlation with outcome. *Ann Oncol.* 2004;15:613-617.

4. Spoo AC, Lubbert M, Wierda WG, Burger JA. CXCR4 is a prognostic marker in acute myelogenous leukemia. *Blood.* 2007;109:786-791.

5. Philipp-Abbrederis K, Herrmann K, Knop S, et al. In vivo molecular imaging of chemokine receptor CXCR4 expression in patients with advanced multiple myeloma. *EMBO Mol Med.* 2015;7:477-487.

6. Lapa C, Luckerath K, Kleinlein I, et al. (68)Ga-Pentixafor-PET/CT for imaging of Chemokine Receptor 4 Expression in Glioblastoma. *Theranostics.* 2016;6:428-434.

7. Avanesov M, Karul M, Derlin T. 68Ga-pentixafor PET: clinical molecular imaging of chemokine receptor CXCR4 expression in multiple myeloma. *Radiologe.* 2015;55:829-831.

8. Gourni E, Demmer O, Schottelius M, et al. PET of CXCR4 expression by a (68)Ga-labeled highly specific targeted contrast agent. *J Nucl Med.* 2011;52:1803-1810.

9. Wester HJ, Keller U, Schottelius M, et al. Disclosing the CXCR4 expression in lymphoproliferative diseases by targeted molecular imaging. *Theranostics.* 2015;5:618-630.

10. Demmer O, Gourni E, Schumacher U, Kessler H, Wester HJ. PET imaging of CXCR4 receptors in cancer by a new optimized ligand. *ChemMedChem.* 2011;6:1789-1791.

11. Meller B, Angerstein C, Liersch T, Ghadimi M, Sahlmann CO, Meller J. (68)Ga-labeled peptides for clinical trials - production according to the German Drug Act: the Gottingen experience. *Nuklearmedizin.* 2012;51:55-64.

12. Martin R, Juttler S, Muller M, Wester HJ. Cationic eluate pretreatment for automated synthesis of [(6)(8)Ga]CPCR4.2. *Nucl Med Biol.* 2014;41:84-89.

13. Kean LS, Sen S, Onabajo O, et al. Significant mobilization of both conventional and regulatory T cells with AMD3100. *Blood.* 2011;118:6580-6590.

14. Brave M, Farrell A, Ching Lin S, et al. FDA review summary: Mozobil in combination with granulocyte colony-stimulating factor to mobilize hematopoietic stem cells to the peripheral blood for collection and subsequent autologous transplantation. *Oncology.* 2010;78:282-288.

15. Zlotnik A, Burkhardt AM, Homey B. Homeostatic chemokine receptors and organ-specific metastasis. *Nat Rev Immunol.* 2011;11:597-606.

16. Jacobson O, Weiss ID. CXCR4 chemokine receptor overview: biology, pathology and applications in imaging and therapy. *Theranostics.* 2013;3:1-2.

17. Nanki T, Hayashida K, El-Gabalawy HS, et al. Stromal cell-derived factor-1-CXC chemokine receptor 4 interactions play a central role in CD4+ T cell accumulation in rheumatoid arthritis synovium. *J Immunol.* 2000;165:6590-6598.

18. Buckley CD, Amft N, Bradfield PF, et al. Persistent induction of the chemokine receptor CXCR4 by TGF-beta 1 on synovial T cells contributes to their accumulation within the rheumatoid synovium. *J Immunol.* 2000;165:3423-3429.

19. Bruhl H, Wagner K, Kellner H, Schattenkirchner M, Schlondorff D, Mack M. Surface expression of CC- and CXC-chemokine receptors on leucocyte subsets in inflammatory joint diseases. *Clin Exp Immunol.* 2001;126:551-559.

20. Uhlen M, Fagerberg L, Hallstrom BM, et al. Proteomics. Tissue-based map of the human proteome. *Science.* 2015;347:1260419.

21. Bruhl H, Cohen CD, Linder S, Kretzler M, Schlondorff D, Mack M. Post-translational and cell type-specific regulation of CXCR4 expression by cytokines. *Eur J Immunol.* 2003;33:3028-3037.

22. Govaert GA, Glaudemans AW. Nuclear medicine imaging of posttraumatic osteomyelitis. *Eur J Trauma Emerg Surg.* 2016;42:397-410.

23. Meller J, Koster G, Liersch T, et al. Chronic bacterial osteomyelitis: prospective comparison of (18)F-FDG imaging with a dual-head coincidence camera and (111)In-labelled autologous leucocyte scintigraphy. *Eur J Nucl Med Mol Imaging.* 2002;29:53-60.

24. Richter WS, Ivancevic V, Meller J, et al. 99mTc-besilesomab (Scintimun) in peripheral osteomyelitis: comparison with 99mTc-labelled white blood cells. *Eur J Nucl Med Mol Imaging.* 2011;38:899-910.

25. Palestro CJ, Love C, Bhargava KK. Labeled leukocyte imaging: current status and future directions. *Q J Nucl Med Mol Imaging.* 2009;53:105-123.

26. Horger M, Eschmann SM, Pfannenberg C, et al. Added value of SPECT/CT in patients suspected of having bone infection: preliminary results. *Arch Orthop Trauma Surg.* 2007;127:211-221.

27. Bar-Shalom R, Yefremov N, Guralnik L, et al. SPECT/CT using 67Ga and 111In-labeled leukocyte scintigraphy for diagnosis of infection. *J Nucl Med.* 2006;47:587-594.

28. Filippi L, Schillaci O. Usefulness of hybrid SPECT/CT in 99mTc-HMPAO-labeled leukocyte scintigraphy for bone and joint infections. *J Nucl Med.* 2006;47:1908-1913.

29. Termaat MF, Raijmakers PG, Scholten HJ, Bakker FC, Patka P, Haarman HJ. The accuracy of diagnostic imaging for the assessment of chronic osteomyelitis: a systematic review and meta-analysis. *J Bone Joint Surg Am.* 2005;87:2464-2471.

30. Jamar F, Buscombe J, Chiti A, et al. EANM/SNMMI guideline for 18F-FDG use in inflammation and infection. *J Nucl Med.* 2013;54:647-658.

31. Meller J, Sahlmann CO, Liersch T, Tang PH, Alavi A. Nonprosthesis Orthopedic Applications of (18)F Fluoro-2-Deoxy-d-Glucose PET in the Detection of Osteomyelitis. *PET Clin.* 2006;1:107-121.

32. Zoccali C, Teori G, Salducca N. The role of FDG-PET in distinguishing between septic and aseptic loosening in hip prosthesis: a review of literature. *Int Orthop.* 2009;33:1-5.

33. Jin H, Yuan L, Li C, Kan Y, Hao R, Yang J. Diagnostic performance of FDG PET or PET/CT in prosthetic infection after arthroplasty: a meta-analysis. *Q J Nucl Med Mol Imaging.* 2014;58:85-93.

34. van der Bruggen W, Bleeker-Rovers CP, Boerman OC, Gotthardt M, Oyen WJ. PET and SPECT in osteomyelitis and prosthetic bone and joint infections: a systematic review. *Semin Nucl Med.* 2010;40:3-15.

35. Michail M, Jude E, Liaskos C, et al. The performance of serum inflammatory markers for the diagnosis and follow-up of patients with osteomyelitis. *Int J Low Extrem Wounds.* 2013;12:94-99.

36. Herrmann K, Schottelius M, Lapa C, et al. First-in-Human Experience of CXCR4-Directed Endoradiotherapy with 177Lu- and 90Y-Labeled Pentixather in Advanced-Stage Multiple Myeloma with Extensive Intra- and Extramedullary Disease. *J Nucl Med.* 2016;57:248-251.

37. Zannettino AC, Farrugia AN, Kortesidis A, et al. Elevated serum levels of stromal-derived factor-1alpha are associated with increased osteoclast activity and osteolytic bone disease in multiple myeloma patients. *Cancer Res.* 2005;65:1700-1709.

38. Bao L, Lai Y, Liu Y, et al. CXCR4 is a good survival prognostic indicator in multiple myeloma patients. *Leuk Res.* 2013;37:1083-1088.

39. Mesguich C, Zanotti-Fregonara P, Hindie E. New Perspectives Offered by Nuclear Medicine for the Imaging and Therapy of Multiple Myeloma. *Theranostics.* 2016;6:287-290.

40. Schauwecker DS. Osteomyelitis: diagnosis with In-111-labeled leukocytes. *Radiology.* 1989;171:141-146.

41. Wukich DK, Abreu SH, Callaghan JJ, et al. Diagnosis of infection by preoperative scintigraphy with indium-labeled white blood cells. *J Bone Joint Surg Am.* 1987;69:1353-1360.

42. Gratz S, Braun HG, Behr TM, et al. Photopenia in chronic vertebral osteomyelitis with technetium-99m-antigranulocyte antibody (BW 250/183). *J Nucl Med.* 1997;38:211-216.

43. Boronat-Ferrater M, Simo-Perdigo M, Cuberas-Borros G, et al. Bone scintigraphy and radiolabeled white blood cell scintigraphy for the diagnosis of mandibular osteomyelitis. *Clin Nucl Med.* 2011;36:273-276.

44. Seabold JE, Simonson TM, Weber PC, et al. Cranial osteomyelitis: diagnosis and follow-up with In-111 white blood cell and Tc-99m methylene diphosphonate bone SPECT, CT, and MR imaging. *Radiology.* 1995;196:779-788.

FIGURES

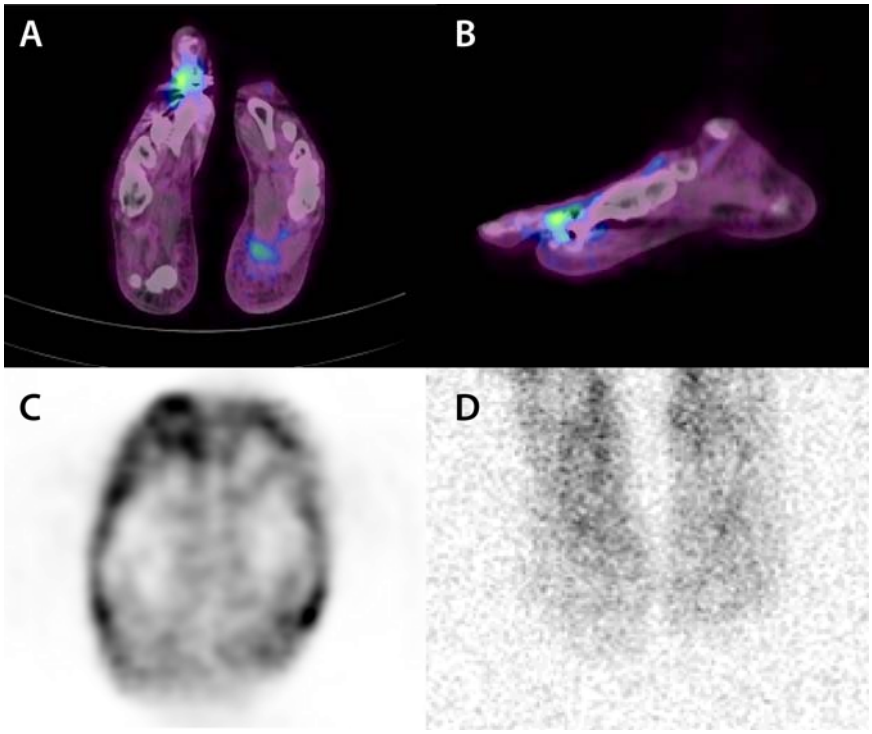

FIGURE 1 INFECTED METATARSOPHALANGEAL PROSTHESIS. 43-years old female patient with elevated CRP 14 months postinterventional. (A-C) ^{68}Ga-Pentixafor-PET/CT shows an elevated tracer uptake at the infected prosthesis at the right metatarsophalangeal joint I. (A) Transversal view of fused ^{68}Ga-Pentixafor-PET/CT. (B) Sagittal view of fused ^{68}Ga-Pentixafor-PET/CT. (C) Transversal view on PET without attenuation correction. Attenuation correction does not influence outcome of ^{68}Ga-Pentixafor-PET/CT by mimicking increased tracer uptake as non-corrected PET images also show an increased uptake around the prosthesis. (D) ^{111}In-oxine scintigraphy was negative. Planar view of ^{111}In-oxine scintigraphy 24h p.i.

FIGURE 2 PLASMOCYTOMA. 62 years old male patient with elevated CRP and suspected sponylodiscites. (A) ^{68}Ga-Pentixafor-PET/CT (sagittal view) showed an increased tracer uptake in multiple vertebrae with a maximum in thoracic vertebrae 10/11. (B) ^{18}F-FDG-PET/CT (sagittal view) showed an increased tracer uptake in multiple vertebrae with a maximum in thoracic vertebrae 10/11. (C) MRI showed a plasmocytoma in thoracic vertebra 10/11.

FIGURE 3 DISTINCT OSTEOMYELITIS AFTER KNEE SPACER IMPLANTATION. 52 years old patient with elevated CRP five months after removal of a total knee arthroplasty and spacer implantation. (A-B) ^{68}Ga-Pentixafor-PET/CT showed an osteomyelitis within the femoral and tibial part of the prosthesis within the right knee. (A) Coronal view of ^{68}Ga-Pentixafor-PET/CT showing an increased tracer uptake in the tibia including the bone marrow compartment. (B) Sagittal view of ^{68}Ga-Pentixafor-PET/CT showing an increased tracer uptake in the femur including the bone marrow compartment. (C) Sagittal view of ^{99m}Tc-besilesomab scintigraphy 4h p.i. showing an osteitis without increased uptake in the bone marrow.

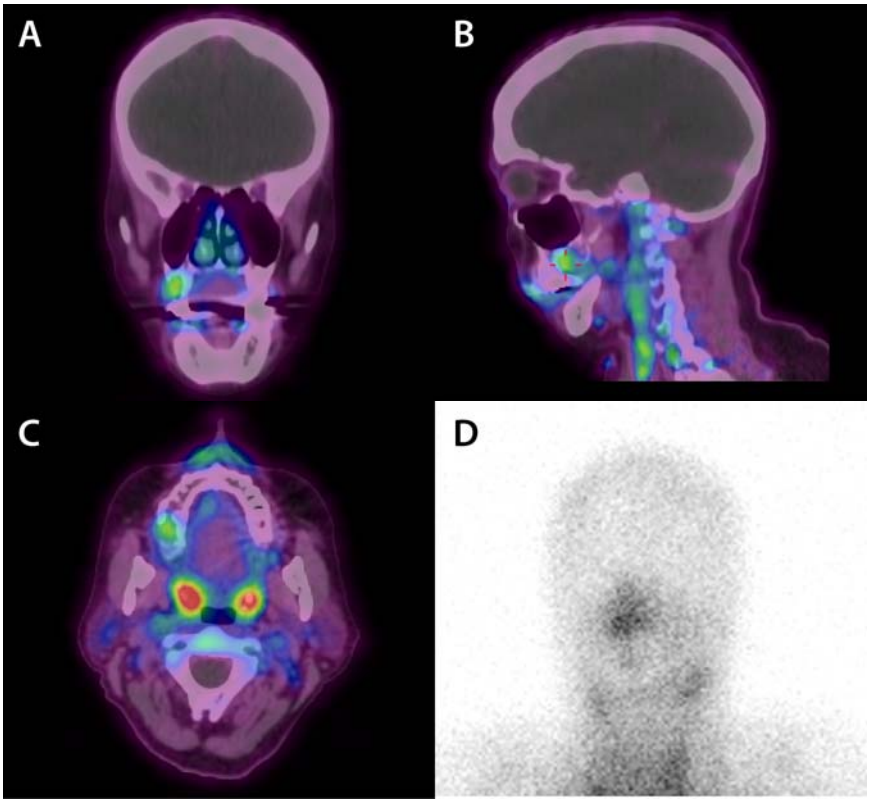

FIGURE 4 OSTEMYELITIS OF THE MAXILLA (REGIO 17). 62-years old female patient 3 months postinterventional. ^{68}Ga-Pentixafor-PET/CT showing an osteomyelitis of the maxilla in Regio 17; coronal (A), sagittal (B) and transversal (C) view. (D) ^{111}In-oxine scintigraphy 24h p.i. with physiological tracer uptake, planar view.

TABLES

TABLE 1 PATIENT CHARACTERISTICS AND RESULTS OF PATIENTS WITH POSITIVE ^{68}GA-PENTIXAFOR-PET/CT . PT=Patient, G=Gender, A= Age, Petixafor= ^{68}Ga-Pentixafor-PET/CT result, FU= follow up, B= bacteriology, P= pathology, MRI= Magnetic Resonance Imaging,

Positive ^{68}Ga-Pentixafor-PET/CT									
PT	**G**	**A**	**Pentixafor**	**Diagnosis**	**Proof**	**SUV_{max}**	**TBR**	**CRP**	**CRP FU**
1	m	21	TP	osteitis femur	B	4.5	10.5	167	neg
2	m	65	TP	osteomyelitis tibia	P	2.2	5.5	neg	neg
3	m	77	TP	infected knee-resurfacing	B	3.9	4.3	neg	neg
4	m	52	TP	osteomyelitis around knee spacer	B	3.5	7	25.4	13.9
5	m	62	FP	necrotic plasmacytoma	MRI, FU	3.6	7.2	10.7	12.1
6	f	43	TP	infected prosthesis meta-tarsophalangeal	FU	2.2	5.5	15	neg
7	f	62	TP	osteomyelitis maxilla	P	3.7	7.4	neg	neg
8	f	51	TP	septic loosening knee endoprosthesis	FU	2.9	7.3	13.3	neg
9	f	73	TP	osteomyelitis mandibula	P	3.4	7.8	47.9	neg

TABLE 1 PATIENT CHARACTERISTICS AND RESULTS OF PATIENTS WITH NEGATIVE ^{68}GA-PENTIXAFOR-PET/CT . PT=Patient, G=Gender, A= Age, Petixafor= ^{68}Ga-Pentixafor-PET/CT result, FU= follow up, CT= Computer Tomograpy,

Negative ^{68}Ga-Pentixafor-PET/CT							
PT	**G**	**A**	**Pentixafor**	**Diagnosis**	**Proof**	**CRP**	**CRP FU**
1	f	61	TN	spondylodesis with broken screw	FU	neg	neg
2	m	19	TN	post-interventional mandible	FU	11.4	neg
3	f	75	TN	aseptic loosening knee endoprosthesis	FU	neg	neg
4	m	78	TN	spondylodesis with broken screw	FU	neg	neg
5	f	48	TN	post-interventional mandible	FU	neg	neg

TABLE 3 COMPARISON OF IMAGING METHODS. PT=Patient, BS= Three-phase bone scintigraphy, FDG=^{18}F-FDG-PET/CT, Indium=^{111}In-oxine labelled leukocyte scintigraphy, Besi= ^{99m}Tc-besilesomab, FU= follow up, B= bacteriology, P= pathology.

Positive ^{68}Ga-Pentixafor-PET/CT								
PT	**Pentixafor PET**	**CT**	**BS**	**FDG**	**Indium**	**Besi**	**MRI**	**Proof**
1	TP	TP	-	TP	-	-	FN	B
2	TP	FN	TP	TP	FN	-	-	P
3	TP	FN	TP	-	TP	-	-	B
4	TP	FN	TP	-	-	TP	-	B
5	FP	FP	-	FP	-	-	TP	FU
6	TP	TP	TP	-	FN	-	-	FU
7	TP	FN	TP	-	FN	-	-	P
8	TP	FN	TP	-	-	-	-	FU
9	TP	TP	TP	-	-	-	-	P
Negative ^{68}Ga-Pentixafor-PET/CT								
1	TN	TN	FP	TN	-	-	-	FU
2	TN	TN	FP	-	-	-	-	FU
3	TN	TN	FP	-	TN	-	-	FU
4	TN	TN	-	-	-	-	-	FU
5	TN	TN	FP	-	TN	-	-	FU

SUPPLEMENTAL MATERIAL

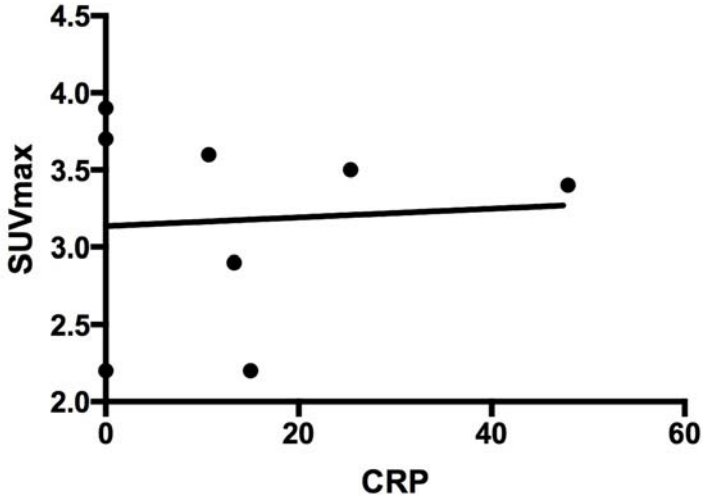

SUPPLEMENTAL FIGURE 1 COMPARISON OF CRP AND SUV_{max}. SUV_{max} did not correlate with CRP levels (r=0.002).